

# Energetics and electronic structure of GaN codoped with Eu and Si

A. Vallan Bruno Cruz, Prashant P. Shinde, and Vijay Kumar\*  
*Dr. Vijay Kumar Foundation, 1969 Sector 4, Gurgaon 122001, Haryana, India*

John M. Zavada

*Department of Electrical and Computer Engineering, North Carolina State University, Raleigh, North Carolina, USA*

(Received 10 November 2011; revised manuscript received 21 December 2011; published 9 January 2012)

First principles calculations using pseudopotentials and generalized gradient approximation (GGA) for the exchange–correlation energy show that addition of Si makes Eu doping in GaN energetically favorable. It breaks local symmetry around Eu ions and leads to shallow states below the conduction band that could facilitate intra- $4f$  shell transitions. Silicon atoms on Ga sites act as intrinsic donors transforming Eu from a  $3+$  to a  $2+$  state. The half-filled  $4f$  states with a  $7 \mu_B$  magnetic moment on each Eu ion lie within the band gap of GaN and are narrower compared with the only-Eu doping case due to reduced hybridization with the host states. There is a tendency for clustering of Eu ions with ferromagnetic coupling and the  $\sim 5\text{-\AA}$  interatomic distance, but EuN phase formation is unfavorable. Further effects of the inclusion of onsite Coulomb interaction  $U$  within GGA+ $U$  formalism on the electronic structure are discussed.

DOI: [10.1103/PhysRevB.85.045203](https://doi.org/10.1103/PhysRevB.85.045203)

PACS number(s): 61.72.uj, 71.15.Nc, 71.55.Eq

## I. INTRODUCTION

Galium nitride is widely used in electronic and optoelectronic devices such as light emitting diodes, blue laser, high electron mobility transistors, display devices, and optical communications.<sup>1–3</sup> Because of its wide band gap, it is an excellent host compared with Si or GaAs for rare earth (RE) dopants such as Eu, Er, and Tm that have bright luminescence in red, green, and blue region, respectively.<sup>4–7</sup> By mixing these dopants, it may be possible to obtain the full visible spectrum. The photoluminescence (PL) by RE ions arises from intra- $4f$  shell transitions that are forbidden in an isolated RE atom due to Laporte selection rules, but they become allowed in RE-doped GaN due to hybridization with the host. The intensity of luminescence strongly depends on the host material, temperature, and impurities that are often present in the host, get created due to doping, or may be intentionally added. In this paper, we report results of *ab initio* calculations to understand the atomic and electronic structure of Eu-doped GaN and the effects of Si codoping that remain open problems.

Europium-doped GaN shows bright emission at 621 nm due to the  $^5D_0 \rightarrow ^7F_2$  transition. In wurtzite GaN, Eu favors substitutional doping at a Ga site in a  $3+$  state. The lack of inversion symmetry around Eu increases the probability for the transition to occur. Analysis based on emission spectra has shown that Eu on a Ga site has an axial  $C_{3v}$  symmetry,<sup>8</sup> but theoretical studies are few.<sup>9,10</sup> Filhol *et al.*<sup>11</sup> studied Eu-, Er-, and Tm-doped GaN by treating RE atoms as trivalent and the remaining  $f$  electrons as part of the core. They found substitution of RE atom on a Ga site to be energetically most favorable. Svane *et al.*<sup>9</sup> used a self-interaction corrected local spin density calculation to study RE doping in cubic GaN. They used small supercells with up to 32 atoms and did not consider atomic relaxation around the dopant. However, as we show, there is significant relaxation around RE atoms that should be treated in a large supercell which is also necessary to treat a low doping concentration of  $\sim 1$  at.%. Sanna *et al.*<sup>12</sup> studied RE-vacancy defect pairs in GaN by local density approximation plus onsite Coulomb interaction  $U$  calculations using a

tight-binding approach. Their analysis showed the RE dopants have a tendency to exist in a divalent state in the presence of defects like N vacancy. The presence of defects near RE ions also reduces the symmetry and thus enhances the intra- $4f$  level transition. In addition, defects could introduce shallow levels, which can act as assistant levels during transition. Doping of Gd has also been studied in GaN, and the possibilities of ferromagnetism and antiferromagnetism have been explored.<sup>13</sup> We consider codoping of Eu and Si in GaN that has been found to enhance luminescence from GaN:Eu<sup>14</sup> by 5–10 times due to the increase in the PL lifetime. Since Si is tetravalent, it is expected to behave as an intrinsic donor when codoped with Eu in GaN. We demonstrate that the addition of Si not only breaks symmetry around Eu ions that would further facilitate intra- $4f$  level transition but also makes Eu doping energetically favorable and leads to narrower  $4f$  states that are likely to improve luminescence from GaN:Eu.

## II. METHOD OF CALCULATIONS

We constructed a  $3 \times 3 \times 3$  supercell of GaN wurtzite structure with 108 atoms, as shown in Fig. 1(a), to study the effects of  $\sim 1$  at.% doping, which is found to be optimal for bright luminescence. Eu and Si atoms have been substituted on Ga sites, and the atomic structure has been fully optimized without using any symmetry until the force on each ion becomes less than  $0.005 \text{ eV/\AA}$ . We use the projector-augmented wave pseudopotential method<sup>15</sup> as implemented in Vienna *ab initio* simulation package code with high precision and generalized gradient approximation (GGA)<sup>16</sup> for the exchange–correlation energy. An energy cutoff of 500 eV is used in all cases for the plane wave expansion, and  $3d$  states of Ga are treated as valence states. The Brillouin zone is sampled by the  $\Gamma$  point for the ionic and electronic optimizations and by Monkhorst and Pack mesh<sup>17</sup> with  $3 \times 3 \times 3$   $k$ -points for the density of states calculations. Spin-polarized calculations have been done for the RE-doped systems, in which case the  $f$  electrons were considered to be valence electrons and treated in a

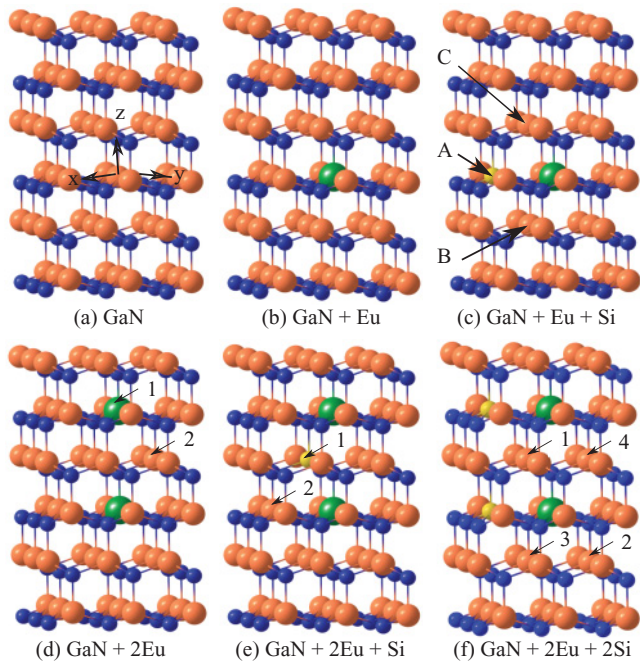


FIG. 1. (Color online) (a) A  $3 \times 3 \times 3$  unit cell of bulk GaN, (b) GaN with a Eu atom on a Ga site, (c) codoping of Eu and Si on Ga sites, (d) two Eu atoms on Ga sites, (e) two Eu and one Si atoms on Ga sites, and (f) two Eu and two Si atoms in the lowest energy configurations. Large light gray (pink), small dark gray (dark blue), large dark gray (green), and small light gray (yellow) balls show Ga, N, Eu, and Si atoms, respectively. (c) A, B, and C show three positions of Si atom that are nearest neighbors of N atoms connected to Eu atom. Site A has the lowest energy. 1 and 2 refer to (d) two positions of Eu and (e) two positions of Si. (f) The lowest energy configuration and other sites (1 and 2), (1 and 3), and (1 and 4) for two Si atoms keeping the Eu sites the same are shown. The coordinate axes are shown in (a).

scalar relativistic way. Further studies have been carried out within GGA+U formalism by including the onsite Coulomb interaction parameter  $U$ . In the literature, the value of the  $U$  parameter has been taken<sup>10,18</sup> in the range of 5–7.4 eV, and for EuO, a value of 7 eV as used by Steeneken *et al.*<sup>18</sup> gives good agreement with experiments. We have taken an effective onsite  $U$  parameter for Eu  $f$  electrons to be 6.0 eV, and the atomic structure has been reoptimized. Tests on different values of  $U$  showed small changes in the positions of the spin-up and spin-down  $4f$  states of Eu.

### III. RESULTS

#### A. Pure GaN

For bulk GaN, the calculated lattice parameters  $a$  and  $c$  are 3.223 and 5.212 Å, respectively, with  $c/a$  value of 1.617 in excellent agreement with the experimental value of 1.624.<sup>19</sup> The calculated cohesive energy (4.373 eV/atom) also agrees well with the experimental value of 4.53 eV/atom. However, the band gap (1.71 eV) is significantly underestimated with respect to the experimental value of 3.4 eV due to the use of GGA. The total, partial, and angular momentum decomposed densities of states are shown in Fig. 2. The  $3d$  states of Ga are nearly completely occupied and have significant hybridization

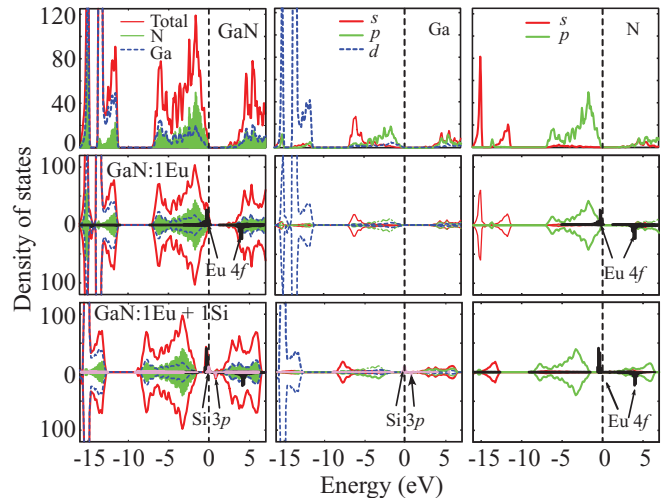


FIG. 2. (Color online) Total (dark gray or red curve), partial (light gray or filled green curve for N and broken curve for Ga) in the left column panels, and angular momentum decomposed electronic densities of states (central and right column panels) for GaN, GaN doped with 1 Eu in the supercell, and GaN codoped with Eu and Si.  $3p$  states of Si and  $4f$  states of Eu are marked. The vertical broken line shows the top of the VB.

with  $2s$  states of N, while the valence band (VB) consists of mainly ( $4s, 4p$ ) states of Ga and  $2p$  states of N.

#### B. GaN doped with Eu

When a Eu atom is doped in GaN on a Ga site [Fig. 1(b)], the ionic relaxation leads to a  $C_{3v}$  symmetry configuration around the doped Eu ion, as also experimentally inferred. There are three Eu-N bonds of the length 2.25 Å and one Eu-N bond of the length 2.30 Å along the  $z$ -axis (symmetry axis) compared with the bulk Ga-N bond length of 1.96 Å. Sanna *et al.*<sup>12</sup> obtained the values of 2.24 and 2.27 Å using a tight binding method. Thus, the doping of a Eu atom in GaN leads to a large ( $\sim 15\%$ ) outward relaxation in the lattice around Eu. Since a Eu ion is bigger than a Ga ion, it leads to deformation of the neighboring lattice structure with the Ga-N bonds nearest neighbor to Eu slightly compressed (bond lengths of 1.92–1.94 Å), while the second and third nearest-neighbor GaN bonds from Eu have values in the range of 1.92–1.98 and 1.94–1.97 Å, respectively. The lattice parameters  $a$  and  $c$  expand slightly to 3.237 and 5.227 Å, respectively, which agrees with the experimental result of Seo *et al.*<sup>20</sup> The doping of a Eu atom in GaN costs 1.84 eV, and the cohesive energy of GaN:Eu decreases due to the deformation of the lattice. We performed a calculation using the optimized atomic configuration of GaN:Eu supercell but replacing the Eu atom with Ga. The strain energy of this configuration is 2.04 eV. Therefore, a small gain occurs due to the chemical bonding when Eu is doped in place of Ga. However, the large deformation energy leads to a net cost.

A single Eu atom doped in GaN on a Ga site behaves like a trivalent atom,<sup>21</sup> as Ga is, and there are six ( $4f$ ) unpaired electrons with a net magnetic moment of  $6 \mu_B$ . The spin-up  $4f$  states lie close to the top of the VB of GaN (Fig. 2) and have a hole. The spin-down unoccupied states lie above the

band gap, in the conduction band (CB) region, and hybridize with the Ga and N states. The band gap for the spin-up states is 1.58 eV. In a more accurate description of the band gap in GaN, such as by the GW method, it has been shown that the bottom of the CB would shift upward;<sup>22</sup> accordingly, the spin-down  $4f$  states could lie close to the experimental CB minimum and hence have weaker hybridization with the GaN states than what is predicted by GGA.

Further calculations on doping of 2 Eu atoms in the supercell ( $\sim 2$  at.% doping) at different positions show that the most favorable positions are the consecutive sites along the  $z$ -axis with a separation of 4.97 Å [position 1 in Fig. 1(d)], as compared to 3.21 Å for the nearest-neighbor Ga-Ga separation in GaN. The total energy of the doped GaN is 3.01 eV higher compared with pure GaN, and Eu doping is again energetically unfavorable. The corresponding strain energy calculated as before by putting two Ga atoms in place of the two Eu atoms is 4.39 eV; therefore, there is higher chemical bonding of Eu atoms in GaN. The effective cost of doping two Eu atoms is 0.67 eV lower than twice the value for one Eu atom. Therefore, a kind of clustering of Eu atoms can be expected, but it is not the formation of EuN, as also inferred from experiments,<sup>20</sup> because position 2 in Fig. 1(d) for the second Eu lies 0.759 eV higher in energy. In the lowest energy configuration, the Eu-N bonds are 2.26 (3 bonds) and 2.33 Å for one Eu atom while for another Eu atom these are 2.26 (3 bonds) and 2.39 Å. The Ga-N bonds nearest to Eu impurity are compressed and have values of 1.91 and 1.95 Å, while the next nearest-neighbor Ga-N bond lengths from Eu are in the range of 1.93–1.94 and are 2.01 Å. The lattice parameters  $a$  and  $c$  further increase to 3.250 and 5.239 Å, respectively, in agreement with the result of Seo *et al.*,<sup>20</sup> who reported a shift in the x-ray diffraction (XRD) peak position to slightly lower angle for 2 at.% Eu doping in GaN. The spin-up  $4f$  states (Fig. 3) have two holes, and there is a 0.84-eV band gap. The spin-down states exhibit a band gap of 1.67 eV, which is not significantly different from the one Eu doping case. The noticeable reduction in the band gap of spin-up states is due to the interaction between the states of two Eu ions in the supercell that makes the band of the  $4f$  states slightly broader. Also, there is low density of states near the bottom of the CB, which decreases the band gap. Such states could facilitate energy transfer from the host to the Eu impurity.

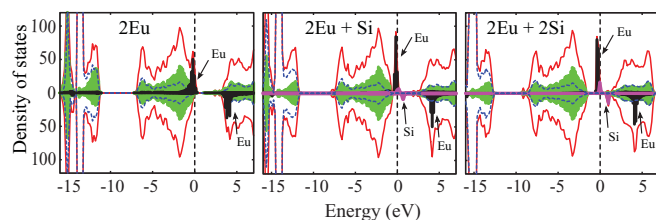


FIG. 3. (Color online) The electronic densities of states for the lowest energy configurations of GaN doped with two Eu in the GaN supercell, two Eu and one Si, and two Eu and two Si, as shown in Fig. 1. The full dark gray (red) curve represents the total density of states. The shaded gray (green), dashed curve, shaded black curve, and shaded light gray (pink) curve represent N, Ga, Eu, and Si partial densities of states, respectively. The vertical broken line shows the top of the VB.

### C. Codoping of Si and Eu in GaN

Codoping of Si can further reduce the symmetry around Eu ions and facilitate intra- $4f$  level transitions. Experimentally,<sup>14</sup> for sufficiently low concentration of Si ( $\sim 0.04$  at.%), PL intensity from GaN:Eu and GaN:(Eu,Si) is very similar. With  $\sim 0.05$  at.% Si, PL intensity increases 5–10 times, and with  $\sim 0.07$  at.% Si concentration, PL emission starts to decrease. Finally, with  $\sim 0.1$  at.% Si concentration, PL emission is  $\sim 1000$  times lower. Around this concentration range of Si, Eu concentration also decreases to similar values and there is a broad band emission in the blue region. Therefore, the amount of Si codoping plays a crucial role in the properties of GaN:Eu. We considered substituting Ga bonded to any of the three basal N atoms neighboring the Eu ion [site A in Fig. 1(c)] and Ga bonded to the neighboring axial N [site C in Fig. 1(c)]. There is another possibility [site B in Fig. 1(c)] that is also the nearest neighbor to basal N. Due to  $C_{3v}$  symmetry of GaN:Eu, sites A and B have different energies and site A is  $\sim 0.68$  eV lower in energy than site B. Also, site A is 0.74 eV lower in energy than the site C. Our calculations show that in the lowest energy configuration, the 4 Eu-N bond lengths are 2.26, 2.28, 2.31, and 2.32 Å. Silicon codoping breaks  $C_{3v}$  symmetry; therefore, this is likely to increase the intra- $4f$  transitions. Uedono *et al.*<sup>23</sup> suggested the possibility of enhancement in transition rate of  $4f$  electrons by stretching the bonds of Eu ions. Furthermore, Si codoping lowers the energy of the supercell by 2.37 eV compared with pure GaN and by 4.22 eV compared with one Eu-doped GaN in the supercell.

We also performed calculations for a Si atom doped on a Ga site in GaN, and it leads to a gain of 3.99 eV, which is lower compared with the energy gain from codoping in GaN:Eu. Therefore, codoping of Si facilitates Eu doping by increasing the stability of the system. For Si doping alone, three Si-N bond lengths are 1.803 Å, while the axial Si-N bond length is 1.796 Å. The Ga-N bonds neighboring to Si expand slightly to 2.03 Å. This is the reverse of the Eu doping case; therefore, Si and Eu codoping can compensate for strain and effectively reduce it. We calculated the strain energy for Eu and Si codoping by substituting Ga on these sites without relaxing the structure: it is 3.89 eV, indicating significant gain by chemical bonding. In the presence of Si, the Eu ion is seen to be divalent. The electronic density of states (Fig. 2) shows the spin-up  $4f$  states to be fully occupied, and there is a net magnetic moment of  $7 \mu_B$ . The additional  $f$  electron pushes the  $4f$  level upward as  $\text{Eu}^{3+}$  changes to  $\text{Eu}^{2+}$ , and all spin-up  $4f$  levels lie in the band gap above the VB of GaN so that they hybridize little with the  $2p$  states of N and appear as sharp, well-defined energy levels. The band gap for the spin-up states reduces to 0.23 eV due to the raising of the  $4f$  states. The optimized lattice parameters  $a$  and  $c$  are 3.235 and 5.219 Å, respectively. Therefore, with Si codoping, there is a very small contraction compared with the one Eu doping case. The Si-N and Eu-N bond lengths are in the range of 1.74–1.82 and 2.26–2.32 Å, respectively, while the Ga-N bonds nearest neighbor and next nearest neighbor to Eu or Si are in the range of 1.90–1.92 Å (from Eu) or 2.03–2.06 Å (from Si) and 1.90–1.97 Å (from Eu) or 1.96–1.99 Å (from Si), respectively. Thus, the Ga-N bond lengths have both elongation and contraction.

We further studied the effects of codoping of one and two Si atoms starting with the lowest energy configuration of two Eu-doped GaN, as representative of low and high concentration of Si codoping. The Si atoms are placed at suitable Ga sites [Figs. 1(e) and 1(f)] so that Si and Eu atoms are connected through common N ions. For one Si codoping, Si is connected to both the Eu ions via N ions [site 1 in Fig. 1(e)]. Also, site 2 in Fig. 1(e) is energetically nearly degenerate with site 1. For two Si codoping, the lowest energy configuration is shown in Fig. 1(f). Configurations with the two Si atoms on (1) + (2) and (1) + (3) lie  $\sim 0.25$  eV higher in energy, while positions (1) + (4) lie 0.35 eV higher than the lowest energy configuration shown in Fig. 1(f). The total energies of the doped systems show Si codoping to be favorable with higher gain of 4.96 eV for two Si atoms compared with 1.44 eV for the codoping of one Si atom. In the latter case, the total number of unpaired  $f$  electrons is 13, and the  $4f$  states lie close to the top of the VB (Fig. 3). The net magnetic moment is  $13 \mu_B$ . For the codoping of two Si atoms, there are 14  $f$  unpaired electrons and the net magnetic moment is  $14 \mu_B$ , indicating ferromagnetic coupling. For only two Eu doping, the net magnetic moment is  $12 \mu_B$ . This is consistent with Si being an intrinsic donor in GaN. The  $4f$  states move up in the band gap in the case of codoping of two Si, as shown in Fig. 3. The Eu-N bond lengths vary from 2.27 to 2.39 Å, while Si-N bond lengths lie in the range of 1.73–1.82 Å. The Ga-N bond lengths near Eu ions are 1.88–1.93 Å and near Si ions are 2.01–2.06 Å, while the remaining bond lengths have a value of  $\sim 1.97$  Å. Similar to the case of one Eu and one Si, hybridization of the occupied spin-up  $4f$  states with the VB is quite small compared to the case of two Eu doping alone. Also, the separation between Eu ions increases to 5.13 Å, and the divalent Eu ions lower the hybridization of the occupied  $4f$  states, thus leading to a weaker interaction between the two Eu ions. Consequently, the peak corresponding to  $4f$  states becomes narrower after Si codoping (Fig. 3). The band gap for the spin-up states for a single codoped Si case is 0.125 eV; for two codoped Si, it is 0.20 eV. There are shallow states near

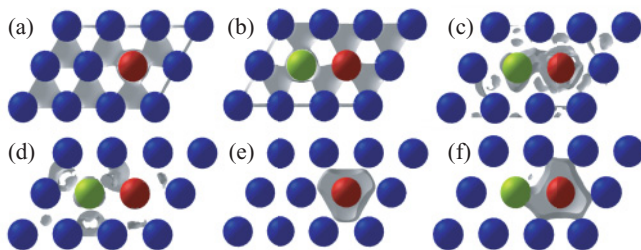


FIG. 4. (Color online) Cuts of the charge density isosurface for (a) one Eu-doped GaN and (b) one Eu and one Si codoped GaN. (c) and (d) Excess and depletion of charge from the difference in the charge density of the doped system and the sum of the charge densities of only GaN, only Eu, and only Si atoms at the respective positions as in the lowest energy configuration of the doped system. (e) and (f) Isosurface of the spin polarization for Eu and Eu+Si-doped GaN, respectively. The polarization is mainly around Eu ion. In this cut, only the cations are seen. Dark gray (blue), medium gray (red), and light gray (green) balls show Ga, Eu, and Si atoms, respectively. The isosurface is shown in a light background color.

the bottom of the CB. Therefore, from these results, we can say that for very low codoping of Si, the effect on PL can be expected to be very small, because the  $4f$  states would remain very close to the top of the VB of GaN. With an increase in Si concentration the  $4f$  states split off the GaN VB maximum, become sharper, and have shallow states. These features could lead to enhancement in PL.

Figures 4(a) and 4(b) show the charge density isosurfaces for GaN:Eu and Si codoped GaN:Eu, and the behavior is similar with covalent bonding. We further calculated the difference in the charge density  $\Delta\rho = \rho(\text{Si codoped GaN:Eu}) - \rho(\text{GaN:Eu})$ , where for Si codoping we considered a configuration of GaN:Eu, in which a Ga atom was substituted in place of Si without relaxing the atomic positions of GaN:Eu. The excess and depletion of charge are shown in Figs. 4(c) and 4(d), respectively. We see excess of charge predominantly around the Eu ion and depletion of charge around the Si ion. These results confirm the divalent character of the Eu ion in the case of Si codoping. Furthermore, Figs. 4(e) and 4(f) show spin polarization for GaN:Eu and Si codoped GaN:Eu. In both cases, the polarization is around the Eu ion.

#### D. GGA+U calculations

Due to the localized character of  $4f$  states, we also studied the effects of onsite Coulomb interaction with an effective  $U$  of 6 eV for Eu  $4f$  electrons. The resulting total, partial, and angular momentum decomposed densities of states for the one Eu doping case, as well as for one Eu and one Si codoping cases, are shown in Fig. 5. A comparison of these results with those shown in Fig. 2 with  $U = 0$  shows that inclusion of  $U$  shifts the spin-up  $4f$  states deeper in the VB and the spin-down  $4f$  states upward in the CB and that these are widespread in the VB and CB. However, when one Si is codoped with one Eu, the occupied spin-up  $f$  levels shift in the band gap and are even sharper compared with the case of  $U = 0$ . The spin-down  $f$  states also become sharper. These results

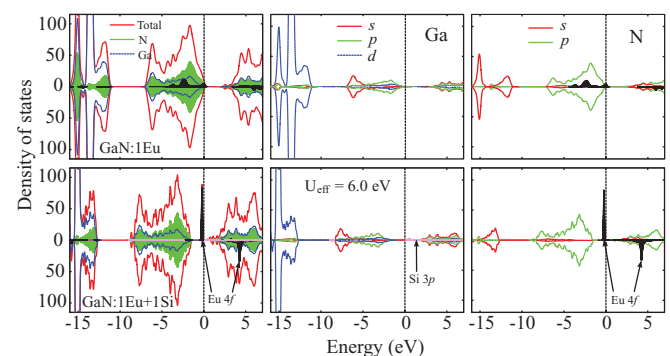


FIG. 5. (Color online) The total, partial, and angular momentum decomposed densities of states for one Eu doping and one Eu and one Si codoping in a GaN supercell within GGA+U formalism with effective  $U = 6$  eV. Eu  $4f$  and Si  $3p$  states for the Eu and Si codoping case are marked. Dark gray (red) curves in the left column panels show the total density of states, while filled gray (green) and broken (blue) curves show N and Ga partial densities of states, respectively. The middle and right column panels show the angular momentum decomposed densities of states for Ga and N, respectively.  $3p$  states of Si are also shown in the middle column, while  $4f$  states of Eu are shown as filled black curve in the right column.

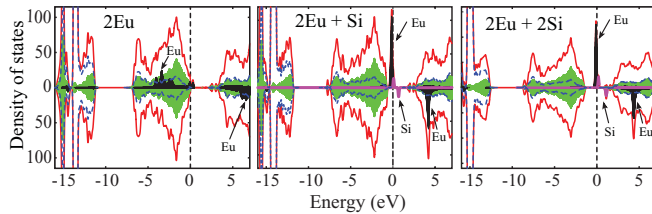


FIG. 6. (Color online) Total and partial densities of states for two Eu, two Eu and one Si, and two Eu and two Si doped in a GaN supercell using GGA+U formalism. The effective  $U$  is taken to be 6 eV. The dark gray (red) curves show the total density of states, while filled gray (green), broken (blue), and filled black curves represent partial densities of states of N, Ga, and Eu, respectively. Filled light gray (pink) curves correspond to Si states. Eu and Si states are also marked with arrows.

show more localization of the half-filled  $4f$  states on Eu with the addition of Si and a decrease in the hybridization with the host states. The total and the partial densities of states for two Eu, two Eu and one Si, and two Eu and two Si cases are shown in Fig. 6. For the case of two Eu doping, the occupied spin-up and the unoccupied spin-down  $f$  states are well distributed in the VB and CB, as we also obtained for the one Eu doping case. The magnetic moment remains  $12 \mu_B$ . When one Si atom is codoped, along with two Eu, the  $f$  states lie close to the top of the VB, because there is one hole in the  $4f$  states and these become quite sharp. The total magnetic moment is  $13 \mu_B$ . Addition of one more Si atom shifts the spin-up  $4f$  states further in the band gap, similar to the case of one Eu and one Si, and both the spin-up and the spin-down states become sharper, as shown in Fig. 6. Therefore, Si codoping again reduces hybridization of Eu  $4f$  states with the host. However, the effect of including  $U$  on the atomic structure is small. The cost of doping one and two Eu in GaN increases by 0.18 and 1.26 eV, respectively. However, with Si codoping,

the energy is lowered by 1.07 and 1.11 eV, respectively, for one Eu and one Si and two Eu and two Si cases, as compared to the case when  $U = 0$ .

#### IV. CONCLUSIONS

We have studied doping of GaN with Eu in a wurtzite phase along with codoping of Si from first principles calculations. We find that Eu doping leads to lowering of the local symmetry, which facilitates intra- $4f$  shell transitions, but it is energetically not favorable. Codoping of Si leads to lowering of energy and a net gain compared with the doping of Eu and Si individually. Therefore, Si codoping is energetically better compared with only-Eu doping. Also, it leads to a further reduction in the local symmetry around the Eu ion compared with Eu alone, and it would enhance intra- $4f$  transitions. Furthermore, even though Eu ions in GaN behave as trivalent species, in the presence of donor dopant Si, Eu ions show a divalent behavior with a  $7 \mu_B$  magnetic moment on each Eu, and these are ferromagnetically coupled for the two Eu doping case. Most significantly, Si codoping reduces hybridization of the  $4f$  states of Eu with the host, making the  $4f$  states sharply defined. This could lead to long life for luminescence, as observed. Also, the electronic structure and the valence state of Eu show significant changes as Si concentration is changed; therefore, it is expected to lead to significant changes in the PL properties, as also observed.

#### ACKNOWLEDGMENTS

We are thankful to the staff of the Centre for Development of Advanced Computing for the use of their supercomputing facilities and excellent support. Support from US Army ITC-PAC Grant No. FA5209-10-P-0219 is gratefully acknowledged.

\*kumar@vkf.in

<sup>1</sup>S. Nakamura, *Science* **281**, 956 (1998).

<sup>2</sup>A. J. Steckl and J. M. Zavada, *MRS Bull.* **24**, 9 (1999).

<sup>3</sup>S. Nakamura, *The Blue Laser Diode: The Complete Story* (Springer, Berlin, 2000).

<sup>4</sup>S. J. Peaton, U. Hommerich, J. T. Seo, R. G. Wilson, and J. M. Zavada, *Appl. Phys. Lett.* **72**, 2710 (1998).

<sup>5</sup>A. J. Steckl, M. Garter, D. S. Lee, J. Heikenfeld, and R. B. Birkhahn, *Appl. Phys. Lett.* **75**, 2184 (1999).

<sup>6</sup>K. Hara, N. Ohatake, and K. Ishi, *Phys. Status Solidi B* **216**, 625 (1999).

<sup>7</sup>D. S. Lee, J. Heikenfeld, R. B. Birkhahn, M. Garter, B. K. Lee, and A. J. Steckl, *Appl. Phys. Lett.* **76**, 1525 (2000).

<sup>8</sup>H. J. Lozykowski, W. M. Jadwisieniczak, J. Han, and I. G. Brown, *Appl. Phys. Lett.* **77**, 767 (2000).

<sup>9</sup>A. Svane, N. E. Christensen, L. Petit, Z. Szotek, and W. M. Temmerman, *Phys. Rev. B* **74**, 165204 (2006).

<sup>10</sup>S. Goumri-Said and M. B. Kanoun, *J. Phys. D Appl. Phys.* **41**, 035004 (2008).

<sup>11</sup>J.-S. Filhol, R. Jones, M. J. Shaw, and P. R. Briddon, *Appl. Phys. Lett.* **84**, 2841 (2004).

<sup>12</sup>S. Sanna, W. G. Schmidt, Th. Frauenheim, and U. Gerstmann, *Phys. Rev. B* **80**, 104210 (2009).

<sup>13</sup>S. M. Nakhmanson, M. Buongiorno Nardelli, and J. Bernholc, *Phys. Rev. B* **72**, 115210 (2005).

<sup>14</sup>R. Wang, Fabrication and Characterization of Gallium Nitride Electroluminescent Devices Co-doped with Rare Earths and Silicon, Dissertation, University of Cincinnati, Cincinnati, 2009), [<http://etd.ohiolink.edu/send-pdf.cgi/Wang%20Rui.pdf?ucin1243025093>]; R. Wang, A. J. Steckl, E. E. Brown, U. Hommerich, and J. M. Zavada, **105**, 043107 (2009).

<sup>15</sup>G. Kresse and D. Joubert, *Phys. Rev. B* **59**, 1758 (1999); P. E. Blöchl, *ibid.* **50**, 17953 (1994).

<sup>16</sup>J. P. Perdew, J. A. Chevary, S. H. Vosko, K. A. Jackson, M. R. Pederson, D. J. Singh, and C. Fiolhais, *Phys. Rev. B* **46**, 6671 (1992).

<sup>17</sup>H. J. Monkhorst and J. D. Pack, *Phys. Rev. B* **13**, 5188 (1976).

<sup>18</sup>G. K. H. Madsen and P. Novák, *Europhys. Lett.* **69**, 777 (2005); A. Rubio-Ponce, A. Conde-Gallardo, and D. Olguin, *Phys. Rev. B* **78**, 035107 (2008); P. G. Steeneken, L. H. Tjeng, I. Elfimov, G. A. Sawatzky, G. Ghiringhelli, N. B. Brookes, and D.-J. Huang, *Phys. Rev. Lett.* **88**, 047201 (2002).

- <sup>19</sup>J. H. Edgar, S. Strite, I. Akasaki, H. Amano, C. Wetzel (Eds.), *Properties, Processing and Applications of Gallium Nitride and Related Semiconductors* (IEE-INSPEC, Hertfordshire, 1999).
- <sup>20</sup>J. Seo, S. Chen, J. Sawahata, M. Mitome, and K. Akimoto, *J. Cer. Proc. Res.* **9**, 68 (2008).
- <sup>21</sup>S. Higuchi, A. Ishizumi, J. Sawahata, K. Akimoto, and Y. Kane-mitsu, *Phys. Rev. B* **81**, 035207 (2010); T. Andreev, N. Q. Liem, Y. Hori, M. Tanaka, O. Oda, D. L. S. Dang, and B. Daudin, *ibid.* **73**, 195203 (2006).
- <sup>22</sup>A. Svane, N. E. Christensen, I. Gorczyca, M. van Schilfgaarde, A. N. Chantis, and T. Kotani, *Phys. Rev. B* **82**, 115102 (2010).
- <sup>23</sup>A. Uedono, H. Bang, K. Horibe, S. Morishima, and K. Akimoto, *J. Appl. Phys.* **93**, 5181 (2003).